IEEE Access
Multidisciplinary | Rapid Review | Open Access Journal

Received July 28, 2018, accepted August 24, 2018, date of publication October 4, 2018, date of current version October 25, 2018.

Digital Object Identifier 10.1109/ACCESS.2018.2868718

Adaptive Subspace Method for Phase Noise Estimation in CO-OFDM Systems

MUYIWA B. BALOGUN, (Graduate Member, IEEE), OLUTAYO OYEYEMI OYERINDE, (Senior Member, IEEE), AND FAMBIRAI TAKAWIRA, (Member, IEEE)

School of Electrical and Information Engineering, University of the Witwatersrand, Johannesburg 2001, South Africa

Corresponding author: Muyiwa B. Balogun (bmbalogun@yahoo.com)

ABSTRACT In this paper, a blind phase noise estimation method for a coherent optical orthogonal frequency-division multiplexing (CO-OFDM) system is considered. Based on the subspace approach, a simple and robust method is proposed to adaptively estimate and track phase noise in CO-OFDM systems. The idea behind this novel technique is to estimate the singular vectors that correspond to the smallest singular values of the noise subspace. A weighting parameter, which is derived based on the forward–backward linear prediction technique, is subsequently constructed using the obtained singular vectors of the noise subspace to adaptively estimate the phase noise in the system. Also, a variable step size is introduced to ensure an improved performance as well as stable convergence. Simulation results are shown to demonstrate the effectiveness as well as the efficiency of the proposed algorithm, which is implemented in a polarization multiplexed CO-OFDM system stressed by polarization mode dispersion, chromatic dispersion, and other polarization-dependent losses along the fiber link.

INDEX TERMS CO-OFDM, OFDM, phase noise estimation, adaptive algorithms, subspace method.

I. INTRODUCTION

High-speed optical networks have become imperative due to the continuous increase in bandwidth-hungry network data services. The coherent optical orthogonal frequency division multiplexing (CO-OFDM) offers several important advantages such as high spectral efficiency, flexibility, and robustness against inter-symbol interference (ISI) [1]–[6]. However, phase noise constitutes a major impairment that degrades the overall reliability, performance and efficiency of the CO-OFDM system. There are various methods that are in existence in the literature, to estimate and compensate the presence of phase noise in CO-OFDM systems. Methods based on pilots as well as data-aided methods have been proposed for phase noise estimation [7]–[10]. These methods have been widely utilized, although they largely result in a high overhead in the optical system. Radio frequency (RF) methods have also been proposed in the literature [11], [12]. Using these methods, it is required that some subcarriers are set aside to form a gap for the RF-pilot insertion. Also, the power of the RF pilot must be optimized in relation to the laser linewidth.

Recently, a number of blind estimation methods, which offer bandwidth efficiency, have been studied and proposed in the literature [13]–[18]. In [14], a decision-directed method, which can be implemented using any modulation format, is proposed. Another method is reported in [15], which is based on blind phase search. The performance of the method in [14] degrades due to error propagation while the method in [15] requires a large number of test phases, leading to a high computational cost and complexity.

In this paper, however, the focus is on the implementation of subspace-tracking based blind phase noise estimation. An efficient adaptive subspace-tracking method is developed and utilized for phase noise estimation in a practical CO-OFDM system. There are various subspace-tracking methods in the literature [19]–[29]. A direct way of estimating a subspace of interest is by applying the singular vector decomposition (SVD) on an observation covariance matrix. The direct SVD approach however results in a high computational complexity. To address this, alternative methods have been studied and proposed [20]–[25]. Most of the alternative methods focus on the signal subspace tracking while little attention is given to the estimation of the noise subspace. A direct modification of the signal subspace, to achieve a low complexity noise subspace tracking is not practicable. This is evident in existing noise subspace tracking

methods, where high instability and inefficiency become inevitable [26]–[29].

The fast data projection method (FDPM) as reported in [30], offers a low complexity, numerically stable, and robust noise subspace tracking. Hence, for the purpose of this study, the subspace-tracking method utilized is based on the FDPM. In order to achieve an adaptive implementation of the FDPM subspace tracking, the selection of the step-size becomes imperative, for the convergence of the algorithm. In [30], utilizing a normalized step-size is proposed. Thus, the speed of convergence and the overall performance of the algorithm largely depend on the stringent selection of the step-size. For an enhanced performance, and to achieve a more stable as well as fast convergence, this work therefore proposes the use of a variable step-size. Also, to obtain a simple adaptive estimate of the phase noise, a prediction parameter is introduced using the forward backward linear prediction (FBLP) technique. The prediction parameter is constructed based on the estimates obtained from the noise subspace-tracking algorithm.

Thus, the main contributions in this paper include the following

1. The derivation and the implementation of an adaptive method based on fast subspace tracking, for phase noise estimation in optical networks. The method utilizes an observation vector that is a subset of the total OFDM subcarrier, in order to adaptively estimate the phase noise, which constantly changes over an OFDM frame. The proposed method is derived and investigated in a practical CO-OFDM system, which considers the impact of dispersions and impairments along the fiber link.
2. Convergence speed and stability are important factors that must be considered while estimating any subspace of interest. Existing subspace methods generally utilizes the regular normalized step-size, which are carefully selected to ensure stability and speed of convergence. This work therefore deviates from the use of the normalized step-size by introducing an adaptive step-size, during the implementation of the noise subspace-tracking algorithm. The unique introduction of the adaptive step-size for use in the subspace-tracking algorithm ensures more stable and faster speed of convergence is achieved while overall system performance is enhanced.
3. To achieve a simple way by which the phase noise can be adaptively obtained based on initial estimates of the subspace-tracking algorithm, a prediction parameter is introduced. The weighting parameter is derived using the forward backward linear prediction (FBLP) technique. The novel combination of the FBLP technique with the subspace-tracking algorithm ensures low-complexity and also improves the robustness of the estimation algorithm. Thus, the proposed approach is called SS-FBLP and the case where the variable step-size is introduced is called SS-FBLP-VSS.

The rest of this paper is organized as follows. Section II presents the CO-OFDM system model. The CO-OFDM system employed is modeled in the presence of phase noise and other pertinent fiber link distortions. Section III discusses the proposed subspace-based adaptive estimation method. Section IV presents a pilot-aided subspace phase noise estimation approach. Section V discuses the computational complexity of the proposed estimation method. Section VI presents the simulation results for the proposed subspace-tracking algorithms. Finally, Section VII gives the conclusion.

II. THE SYSTEM MODEL

Considering the transceiver structure of a typical CO-OFDM system, the binary inputs to the RF-OFDM transmitter are encoded, before the serial-to-parallel conversion. The converted data are then mapped and converted into time domain signals by the inverse fast Fourier transforms (IFFT) operation. The resulting signals are digital-to-analog converted where the low pass filter is utilized, to address aliasing. At the RF-to-optical up-converter block, the transmit signal is transformed from the electrical domain to the optical domain using an optical in-phase/quadrature (IQ) modulator, which consists of two Mach-Zehnder modulators (MZMs) with a 90 degree phase offset as shown in Fig. 1 [6].

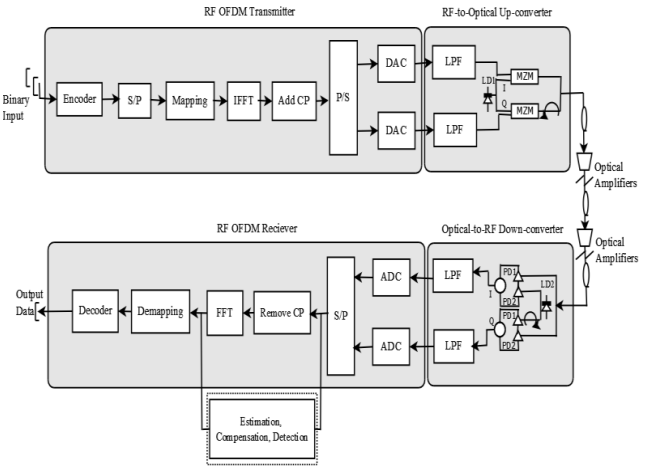

FIGURE 1. Block diagram of the CO-OFDM transceiver.

Thus, the baseband transmitted OFDM signal after IFFT is expressed below as:

$$x_i(n) = \frac{1}{\sqrt{N}} \sum_{m=0}^{N-1} X_i(m) e^{\frac{j2\pi nm}{N}}. \quad (1)$$

where $x_i(n)$ denotes the n^{th} sample of the i^{th} OFDM symbol, N represents the total number of subcarriers, while $X_i(m)$ denotes the data symbol transmitted on the m^{th} data subcarrier. The received OFDM baseband signal in time domain is expressed as:

$$y_i(n) = e^{j\rho_i(n)} \left[x_i(n) \otimes \Gamma^{-1}(Z(m)) \right] + g_i(n) \quad (2)$$

where $\Gamma^{-1}(\cdot)$ and $\otimes$ represent the IDFT operation and the circular convolution respectively. The total amplified spontaneous emission (ASE) noise generated from inline optical amplifiers is represented as $g_i(n)$, while $Z(m)$ denotes the channel impulse response of the fiber link encompassing the polarization mode dispersion, as well as other polarization dependent losses (PDLs) [31], [32]. Thus, $Z(m)$ can be expressed mathematically as [6]:

$$Z(m) = e^{j\emptyset(m)} \prod_{p=1}^{M} exp\left\{\left(-\frac{1}{2}j \cdot \overrightarrow{\beta_p} \cdot f_m + \frac{1}{2}\overrightarrow{\omega_p}\right) \cdot \overrightarrow{\lambda}\right\} \quad (3)$$

where the number of the PMD/PDL cascading elements in the entire fiber link is denoted as M, with each section represented by its birefringence vector $\overrightarrow{\beta_p}$ and PDL vector $\overrightarrow{\omega_p}$ as detailed in [6]. The term $\vec{\lambda}$ connotes the Pauli's vector, assuming quadratic dependence on frequency while $\emptyset(m)$ is the group velocity dispersion (GVD), which is given as:

$$\emptyset(m) = \pi \cdot c \cdot q_f \cdot \frac{f_m^2}{f_o^2}, \quad (4)$$

As expressed above, $\emptyset(m)$ is primarily a phase shift due to distortion in the fiber link, where q_f denotes the chromatic dispersion in the link, f_m is the frequency for the m^{th} subcarrier and f_o is the center optical frequency. Also, the laser phase noise in the optical system $\rho_i(n)$ is described as a Weiner-Levy process, which can be expressed mathematically as [13]:

$$\rho_i(n) = \rho_{i-1}(N-1) + \sum_{v=-N_{CP}}^{n} s(i(N+N_{CP})+v), \quad (5)$$

where $s(v)$ is the independently incremental movement of the phase noise at time instant v, which is Gaussian distributed with zero mean and variance $\sigma^2 = 2\pi h T_s$, where h represents the combined laser linewidth of the transmitter and the receiver lasers, while N_{CP} connotes the cyclic prefix (CP) length and T_s is the symbol period.

The FFT is performed to recover the received OFDM information symbol, which is given as [33], [34]:

$$Y_i(m) = B_i(0) X_i(m) Z(m) + \sum_{k=0,k\neq m}^{N-1} X_i(k) Z(k) B_i(k-m) + G_i(m), \quad (6)$$

where $B_i(m)$ is a function of the distortion due to the laser phase noise, which can be expressed as [10]:

$$B_i(m) = \frac{1}{N}\sum_{n=0}^{N-1} e^{j\rho_i(n)} \cdot e^{\frac{j2\pi nm}{N}} \quad (7)$$

$$B_i(0) = \frac{1}{N}\sum_{n=0}^{N-1} e^{j\rho_i(n)}, \quad (8)$$

which is approximated as

$$B_i(0) \cong |B_i(0)|. \quad (9)$$

It denotes the phase evolution, which corresponds to the time-average of the laser phase noise over the i^{th} OFDM symbol and Φ_i is considered as the common phase error (CPE) given as [13]:

$$\Phi_i = \angle B_i(0) \quad (10)$$

The overall interference including the residual interference in the system is given by

$$ICI_i(m) = \sum_{k=0,k\neq m}^{N-1} X_i(k) \cdot Z(k) \cdot B_i(k-m). \quad (11)$$

where

$$B_i(k-m) = \sum_{n=0}^{N-1} e^{j\rho(n)} \cdot e^{\frac{j2\pi n(k-m)}{N}}. \quad (12)$$

Also, the effective signal-noise-ratio at the detector is expressed as [35]:

$$SNR' = \frac{E\{B_i(0) X_i(m) Z(m)\}^2}{E\{ICI_i(m)\}^2 + E\{G_i(m)\}^2} = \frac{\sigma_x^2 Z^2(m)}{\sigma_x^2 \sum_{k=0,k\neq m}^{N-1} B_i^2(k-m) Z^2(k) + \sigma_G^2}, \quad (13a)$$

$$SNR' = \frac{Z^2(m)}{\sum_{k=0,k\neq m}^{N-1} B_i^2(k-m) Z^2(k) + \frac{\sigma_G^2}{\sigma_x^2}}, \quad (13b)$$

$$SNR' = \frac{Z^2(m)}{\sum_{k=0,k\neq m}^{N-1} B_i^2(k-m) Z^2(k) + SNR^{-1}}, \quad (13c)$$

where σ_x^2 is the variance of the transmitted information signal and σ_G^2 is the variance of the ASE noise, while $SNR = \frac{\sigma_x^2}{\sigma_G^2}$ is the original channel SNR without the effect of $ICI_i(m)$ [35]. The SNR is related to the optical SNR (OSNR) by the expression [4]

$$OSNR(dB) = 10\log_{10}[SNR] + 10\log_{10} {}^{B_f}/_{R_s}, \quad (14)$$

where B_f is the central bandwidth while R_s is the symbol rate [4].

From the expressions in (6)-(14), the received signal can be analyzed and the impact of the phase noise can be estimated, evaluated and compensated.

III. THE PROPOSED SUBSPACE-BASED ADAPTIVE ESTIMATION METHOD

A. THE SUBSPACE PROBLEM

The subspace problem is generally approached by assuming a condition where the parameter to be estimated remains constant over the entire OFDM frame. However, such assumption may not hold in the case of phase noise, which is constantly changing within an OFDM frame. In order to overcome the difficulty of adaptively estimating the phase noise, an observation vector, which is a subset of the total OFDM subcarrier, is utilized. The observation vector is defined as a portion of the received signal, which is denoted as $Y(j)$ with length L,

where $L < N$. This enables the frequently changing phase noise to be effectively estimated across $Y(j) \ldots .. Y(L+j)$. Hence, the observation sequence on which the phase noise subspace tracking problem is based can be defined as

$$\boldsymbol{S}_j = \left[S_j(1) \ldots \ldots .S_j(L)\right] = \left[Y(j) \ldots .. Y(L+j)\right], \quad (15)$$

Therefore considering a non-negative covariance $\boldsymbol{P}$ with size L, of the received data sequence $\boldsymbol{S}_j$, by applying singular value decomposition on $\boldsymbol{P}$, the following expression is obtained

$$\boldsymbol{P} = \mathbb{E}\left[\boldsymbol{S}_j \boldsymbol{S}_j^H\right] = \boldsymbol{U}\boldsymbol{\Lambda}\boldsymbol{U}^H \quad (16)$$

where $\Lambda = diag\{\gamma(1), \ldots \ldots \ldots \gamma(L)\}$ denotes the diagonal matrix of singular values of $\boldsymbol{P} = \mathbb{E}[\boldsymbol{S}_j \boldsymbol{S}_j^H]$, whose elements are the singular values of $\boldsymbol{P}$ satisfying $\gamma(1) \geq \gamma(2) \geq \ldots . \geq \gamma(D) > \gamma(D+1) \geq \ldots . \gamma(L) \geq 0$ while $\boldsymbol{U}$ contains the corresponding singular vectors with elements $u(1) \ldots .u(L)$. A simple orthogonal iterative method can be used to estimate the subspace of interest, to obtain the singular vectors corresponding to the singular values of the matrix $\boldsymbol{P}$. Since L represents the rank of the subspace of interest, then the sequence of matrices $\boldsymbol{U}(j)$ is described by the iteration [36]

$$\boldsymbol{U}(j) = orthonorm\{\boldsymbol{P}\boldsymbol{U}(j-1)\}, \quad j = 1, 2, \ldots . \quad (17)$$

where orthonorm represents an orthogonal procedure using the QR decomposition, and given that the matrix $\boldsymbol{U}^H(j)[u(1) \ldots .. u(D)]$ is not singular, then

$$\lim_{i \to \infty} \boldsymbol{U}(j) = [u(1) \ldots .. u(D)]. \quad (18)$$

As mentioned above, since the aim is to estimate the subspace that contains the smallest singular values corresponding to the smallest singular vectors, two variants of the orthogonal iteration are presented. These orthogonal iterative methods ensure the realization of such estimates and also enable adaptive implementations. The variants are described below [36]

$$\boldsymbol{U}(j) = orthonorm\left\{\boldsymbol{P}^{-1}\boldsymbol{U}(j-1)\right\}, \quad (19)$$

$$\boldsymbol{U}(j) = orthonorm\{(I_L - \mu\boldsymbol{P})\boldsymbol{U}(j-1)\}, \quad j = 1, 2, \ldots \quad (20)$$

where $\mu > 0$ is the step-size, which is relatively small, while I_L is the identity matrix. For the purpose of this work, (20) will be adopted since it has a lower complexity compared to (19), which yields a higher complexity due to the matrix inversion.

In order to achieve an adaptive implementation at an instance where $\boldsymbol{P}$ is not available, the received vector is obtained sequentially and the matrix $\boldsymbol{P}$ can be substituted with an adaptive estimate $\hat{\boldsymbol{P}}_j$, which satisfies the condition $E\left[\hat{\boldsymbol{P}}_j\right] = \boldsymbol{P}$. An orthogonal iterative process is then used to compute the singular vectors associated with its singular values. The adaptive orthogonal iterative algorithm is expressed as:

$$\boldsymbol{U}(j) = orthonorm\left\{(I_L - \mu\hat{\boldsymbol{P}}_j)\boldsymbol{U}(j-1)\right\}. \quad (21)$$

The parameter μ used above represents the constant step-size. However, to achieve a better stability and speed of convergence, an adaptive step-size $\mu(j)$ is utilized, which is defined as [37]:

$$\mu(j) = \delta \cdot \text{erf}\left(1 - e^{-\alpha|\tau_j|}\right), \quad (22)$$

where $\text{erf}(x) = 2/\sqrt{\pi} \int_0^x e^{-\sigma^2} \partial\sigma$, represents the error function operation. The variation rate of the adaptive step-size is controlled by adjustment factors δ and α, while $\tau_j = B_j - B_{j-1}$ is the error term. Also, the range of $\mu(j)$ is given as $0 < \mu(j) < 2/\gamma(1)$, where $\gamma(1)$ is the maximum singular value of the covariance matrix. Also, the range of δ is within the boundary $0 < \delta < 2/\gamma(1)$ given that $0 < \text{erf}\left(1 - e^{-\alpha|\tau_j|}\right) < 1$.

B. THE PREDICTION PARAMETER

As $\boldsymbol{U}(j)$ is obtained using the adaptive iterative method, its corresponding L columns with vectors $[u(1) \ldots .. u(D)]$ are therefore utilized to construct the prediction parameter $\boldsymbol{W}$. In order to achieve this, a method based on the minimum-norm solution of the forward-backward linear property in [38], is employed. Using the singular values as well as the singular vectors of the estimate $\boldsymbol{U}(j)$, the relationship between the prediction parameter and the covariance matrix is derived. Therefore, considering a linear prediction parameter described by the column vector $\boldsymbol{W}_j$

$$\boldsymbol{W}_j = \left[w_j(1), w_j(2) \ldots \ldots w_j(D)\right]^T, \quad (23)$$

with $[.]^T$ denoting transpose and $D \leq L$. Utilizing the prediction parameter in both forward and backward direction, the prediction equation can be expressed as [38]:

$$\begin{bmatrix} S_j(D) & S_j(D-1) & \ldots S_j(1) \\ S_j(D+1) & S_j(D) & \ldots S_j(2) \\ \vdots & \vdots & \vdots \\ S_j(L-1) & S_j(L-2) & \ldots S_j(L-D) \\ S_j^*(2) & S_j^*(3) & \ldots S_j^*(D+1) \\ S_j^*(3) & S_j^*(4) & \ldots S_j^*(D+2) \\ \vdots & \vdots & \vdots \\ S_j^*(L-D) & S_j^*(L-D+1) & S_j^*(L) \end{bmatrix} \begin{bmatrix} w_j(1) \\ w_j(2) \\ \vdots \\ w_j(D) \end{bmatrix}$$

$$= -\begin{bmatrix} S_j(D+1) \\ S_j(D+2) \\ \vdots \\ S_j(L) \\ \ldots \ldots \ldots \ldots \\ S_j^*(1) \\ S_j^*(2) \\ \vdots \\ S_j^*(L-D) \end{bmatrix}, \quad (24)$$

which can be written in a simpler form as:

$$\boldsymbol{R}_j \boldsymbol{W}_j = -\boldsymbol{a}_j \quad (25)$$

Thus, the minimum-norm solution to the expressions in (23)-(24) is expressed as:

$$\boldsymbol{W}_j = -\boldsymbol{R}_j^{-1}\boldsymbol{a}_j, \tag{26}$$

where $\boldsymbol{R}_j^{-1}$ denotes the pseudo-inverse of $\boldsymbol{R}_j$, which can be expressed as

$$\boldsymbol{R}_j^{-1} = (\boldsymbol{R}_j^{*}\boldsymbol{R}_j)^{-1}\boldsymbol{R}_j^{-1}. \tag{27}$$

Also, given

$$\boldsymbol{P} = \boldsymbol{R}_j{}^{*}\boldsymbol{R}_j; \hat{\boldsymbol{P}}_j = -\boldsymbol{R}_j{}^{*}\boldsymbol{a}_j, \tag{28}$$

in linear prediction representation, where $\boldsymbol{P}$ is the correlation matrix and $\hat{\boldsymbol{P}}_j$ is the correlation vector determined from the received data sequence while "*" denotes complex conjugate transpose. From (28), the prediction parameter $\boldsymbol{W}_j$ can be expressed as:

$$\boldsymbol{W}_j = (\boldsymbol{R}_j^{*}\boldsymbol{R}_j)^{-1}\boldsymbol{R}_j^{-1}\cdot\boldsymbol{a}_j \Rightarrow \boldsymbol{W}_j = \boldsymbol{P}^{-1}\hat{\boldsymbol{P}}_j. \tag{29}$$

Therefore from (29) and recalling the SVD expression in (15) and (16) above, the prediction parameter is obtained as:

$$\boldsymbol{W}_j = \sum_{l=1}^{D}\frac{u(l)}{\gamma(l)}\cdot\left(u^{H}(l)\cdot\hat{\boldsymbol{P}}_l\right). \tag{30}$$

As $u(l)$ is the efficient estimates of the singular vectors, $\boldsymbol{W}_j$ also constitutes the estimate of the singular vectors corresponding to the smallest singular values of the subspace of interest. Thus, the adaptive phase noise estimation is therefore obtained using (20), which is expressed as:

$$\hat{B}_j = normalize\left\{\hat{B}_{j-1} - \mu\cdot w_j(1)\hat{B}_{j-1}\right\}, \tag{31}$$

$$\hat{\Phi}_j = \angle\hat{B}_j, \tag{32}$$

where $\angle$ represents the phase angle. Finally, the compensation is obtained using the following expression

$$\hat{\boldsymbol{Y}}(j) = e^{-j\hat{\boldsymbol{\Phi}}_j}Y(j) \tag{33}$$

Thus, the relation between the prediction parameter and the covariance vector is shown. Also, it is seen that the prediction parameter is a linear combination of the singular vectors of the subspace of interest.

IV. PILOT AIDED SUBSPACE PHASE NOISE ESTIMATION

In this section, a variation of the subspace method is presented, where pilots are used to obtain the initial phase for the expression in (31). Now considering the case where M_p pilot subcarriers are introduced, and $\{m_1, m_2, \ldots m_{M_p}\}$ of pilot tones are available at each payload OFDM symbol. The phase is estimated based on pilot subcarriers in OFDM symbols. Hence, the following expression is obtained:

$$\acute{B}(0) = \frac{1}{M_p}\sum_{m\in\{m_p\}}\frac{Y(m)\,|X(m)|}{X(m)\,|Y(m)|}. \tag{34}$$

Hence, the $\acute{B}(0)$ obtained from (34) is used to compensate the signal and the following is obtained

$$Q(m) = Y(m)\,\acute{B}(0). \tag{35}$$

The sequence for the subspace algorithm with pilot subcarriers becomes $\boldsymbol{S}_j = [S_j(1)\ldots\ldots S_j(L)] = [Q(j)\ldots..Q(L+j)]$. Therefore, the non-negative covariance $\boldsymbol{P}$ with size L, of the received data sequence $\boldsymbol{S}_j$, by applying singular value decomposition, is obtained by $\boldsymbol{P} = \mathbb{E}[\boldsymbol{S}_j\boldsymbol{S}_j^{H}] = \boldsymbol{U}\boldsymbol{\Lambda}\boldsymbol{U}^{H}$.

In the subspace adaptation, the initial value of the phase can be set as a random value or using $\acute{B}(0)$ in (34), before the final estimation is obtained using the subspace approach as described from (16)-(33). Results show that phase initialization using $\acute{B}(0)$ ensures a better performance.

Also, the relationship between the prediction parameter and the covariance vector is shown in (23)-(29). It is seen that the prediction parameter is a linear combination of the singular vectors of the subspace of interest.

TABLE 1. Computational complexity of the subspace methods.

Subspace Method	Multiplication	Addition
SVD	$L^2(L+2D+2)$	$L(3D^2+2D)$
SS-FBLP	$L(3D+1)$	$L(5D+1)$
SS-FBLP-VSS	$L(5D+2)$	$L(7D+2)$

V. COMPUTATIONAL COMPLEXITY

Using the direct SVD, the number of operations required is generally of order $O(L^3)$ [30]. The SVD method generally results in high computational complexity with $L^2(L+2D+2)$ multiplication operations and $L(3D^2+2D)$ addition operations [30]. However, the proposed method, which is based on the FDPM approach, using the normalization process described in Table 2, ensures a reduced complexity. The sequence $\{\boldsymbol{U}(j) = norm[\boldsymbol{H}(j)]\}$ have computational complexity of $O((L+D)D)$ since the normalization of a vector requires $O(L+D)$ operations. Using the normalization operation ("norm") reduces the complexity and ensures that an order of magnitude is gained as the use of the "orthonormalize" operation is of complexity $O((L+D)^2D)$ [36]. Thus, the proposed SS-FBLP method requires $L(3D+1)$ multiplication operations and $L(5D+1)$ addition operations. Also, considering the adaptive estimator in (31), the complexity is of order $O(D^2)$ due to the fact that the adaptive expression in (20) is used rather than (19). Using (19) would have resulted in $O(D^3)$ due to the matrix inversion [36]. The comparison of the considered subspace methods in terms of the required multiplication and addition operations is presented in Table 1. Also, the complexity graph of the subspace methods in comparison with the SVD method is presented in Fig. 11. It can be seen that the proposed methods come with a much lower computational complexity in comparison with the direct SVD method. The summary of the phase noise estimation algorithm is as shown in Table 2.

TABLE 2. Summary of the Proposed Estimation Algorithm.

- For $i = 1,2, \ldots \ldots 10^3$
- For $m = 1,2, \ldots \ldots N$
- Compute $Y_i(m)$ using (6)
- End for
- For $j = 1,2, \ldots \ldots L; L < N$
- Obtain sequence $\boldsymbol{S}_j = [S_j(1) \ldots \ldots S_j(L)] = [Y(j) \ldots \ldots Y(L+j)]$
- Obtain covariance $\boldsymbol{P} = \mathbb{E}[\boldsymbol{S}_j \boldsymbol{S}^H{}_j]$
- Obtain $\boldsymbol{U}(j) = orthonorm\{\boldsymbol{P}\boldsymbol{U}(j-1)\}$, using the FDPM approach.
- Initialize with a random orthonormal matrix $\boldsymbol{U}(0)$
- Available from previous instant: $\boldsymbol{U}(j-1)$
- Compute μ
- $\boldsymbol{c}(j) = \boldsymbol{U}^H(j-1)\boldsymbol{S}_j$
- $\boldsymbol{T}(j) = \boldsymbol{U}(j-1) \pm \mu \boldsymbol{S}_j \boldsymbol{c}^H(j)$
- $\boldsymbol{b}(j) = \boldsymbol{c}(j) - \|\boldsymbol{c}(j)\|\boldsymbol{e}'$, *where* $\boldsymbol{e}' = [\boldsymbol{10}, \ldots . \boldsymbol{0}]^T$
- $\boldsymbol{H}(j) = \boldsymbol{T}(j) - \frac{2}{\|\boldsymbol{b}(j)\|^2}[\boldsymbol{T}(j)\boldsymbol{b}(j)]\boldsymbol{b}^H(j)$
- $\boldsymbol{U}(j) = norm[\boldsymbol{H}(j)]$, where norm[.] is the normalization of each column of $\boldsymbol{H}(j)$
- Obtain singular vectors $[u(1) \ldots . . u(D)]$ from $\boldsymbol{U}(j)$ for the construction of $\boldsymbol{W}_j$
- Construct the weighting parameter $\boldsymbol{W}_j = \sum_{l=1}^{D} \frac{u(l)}{\gamma(l)} . \left(u^H(l) . \widehat{\boldsymbol{P}}_l\right)$ using (30)
- Compute $\hat{B}_j$ using (31)
- Compute $\widehat{\Phi}_j$ using (32)
- End for
- Compute MSE

End.

VI. SIMULATION AND DISCUSSION

The performance of the proposed algorithm is investigated in a 20 *Gb/s* CO-OFDM system. In the simulation, the sampling frequency of the OFDM symbol is 28.8*ns*, with IFFT/FFT chosen as 256, $L = 128$, $D = 96$ while a 12.5% cyclic prefix is used. The quadrature phase shift keying modulation format is adopted. The practical fiber link consists of ten spans of 80*km* standard single mode fiber (SSMF) with fiber dispersion $17ps/km/nm$, differential group delay of $5ps/\sqrt{km}$ as well as loss coefficient of $0.2dB/km$. A total number of 1000 OFDM symbols is used for each bit-error-rate simulation. Also optical amplifier, EDFA has 16*dB* gain with noise figure of 4*dB* and the non-linear coefficient of the fiber is $1.32/W/km$. The parameters are as shown in Table 3.

The FDPM subspace-tracking algorithm as described in Table 2 depends on the selection of the step-size for stability and convergence. In [30], it has been suggested that a value close to unity ensures the needed stability and speed of convergence. Therefore, with the range $0 < \mu < 1$, the constant step-size parameter is varied in this simulation between values 0.90 and 1.0, to ascertain the most suitable value for the SS-FBLP method. Fig 2 shows the mean square error (MSE) plot for the SS-FBLP method, with varied values of step-size. The MSE of the phase noise is defined as MSE $= \mathbb{E}\left[\left|\angle\hat{B}_j - \angle B_j\right|^2\right]$. Although the step-size value $\mu = 1.0$ gives a desirable performance especially for lower values

TABLE 3. Simulation parameters.

Parameters	Specifications
FFT size	256
Modulation format	QPSK
Data rate	20 Gb/s
Cyclic prefix	12.5 %
Sampling frequency	28.8 ns
Fiber dispersion	17 ps/km/nm
Differential group delay	5 ps/$\sqrt{}$km
Loss coefficient	0.2 dB/km
Wavelength	1550 nm
Amplifier gain	16 dB
Noise figure	4 dB
Non-linear fiber coefficient	1.32/W/km

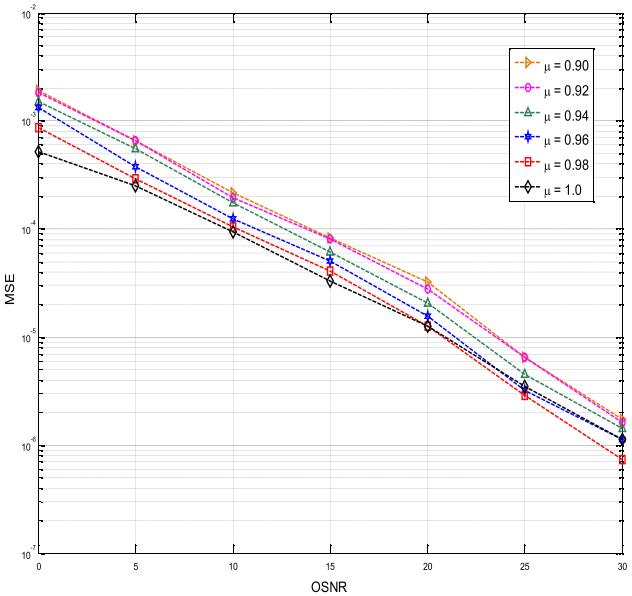

FIGURE 2. MSE versus SNR plot for the SS-FBLP method with varied values of the step-size μ.

TABLE 4. Acronyms and description of techniques.

ACRONYM	DESCRIPTION OF TECHNIQUE
SVD	Singular Vector Decomposition
SS-FBLP	Subspace Forward Backward Linear Projection Technique
SS-FBLP-VSS	Subspace Forward Backward Linear Projection Variable Step Size Technique

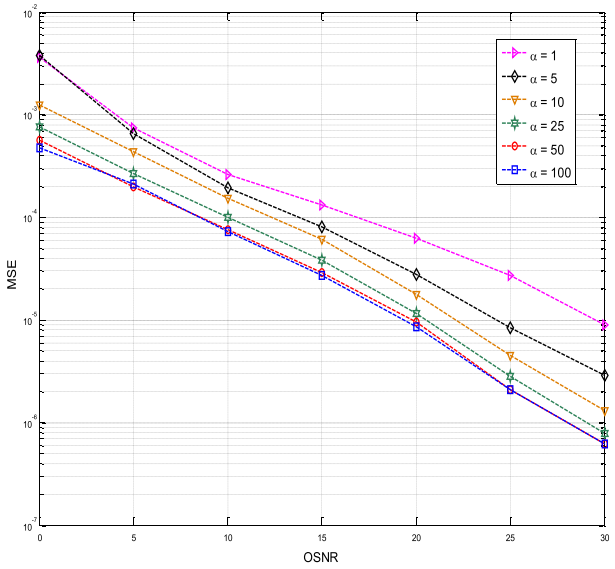

FIGURE 3. MSE performance of the SS-FBLP-VSS method with varied values of the adjustment variable α.

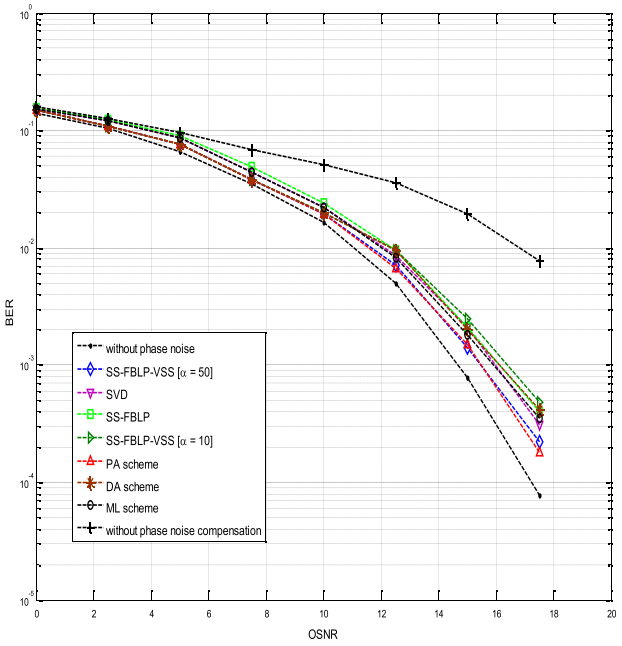

FIGURE 4. BER sensitivity for the proposed estimation algorithms in comparison with the direct SVD method.

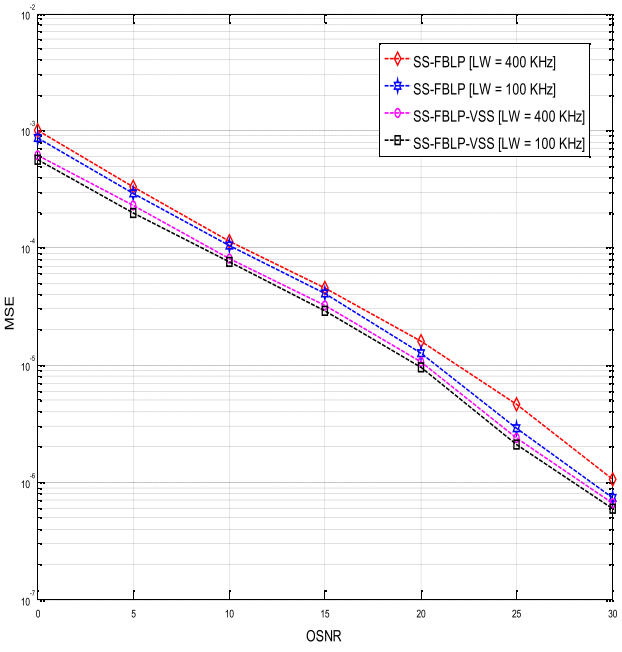

FIGURE 5. MSE performance of the proposed algorithms with linewidth set to 100 KHz and 400 KHz.

of SNR, the preferred selection is $\mu = 0.98$, due to the consistent and stable MSE performance offered across all the values of SNR. Hence, the step-size value $\mu = 0.98$ will be utilized for subsequent analysis of the SS-FBLP method. Also, the introduced adaptive step-size as described in (22) brings new dynamics such as the selection of the appropriate value for the adjustment variables δ and α. For the purpose of this study, the value of the variable δ is set to unity i.e. $\delta = 1$, to achieve good steady-state performance. The value selected for the factor α has a more prominent influence on the variation rate of the step-size and the overall stability of the SS-FBLP-VSS method. Thus, the most suitable selection for α is investigated as shown in Fig. 3, where the value of α is varied starting from $\alpha = 1$. It becomes evident that the MSE performance is improved as the value of α increases. However, at some point, the MSE performance ceases to show any further marked improvement. Hence, the selection of $\alpha = 50$ is considered appropriate and will be used for the subsequent analysis and comparison with the SS-FBLP method.

Fig. 4 shows the BER performance of the proposed SS-FBLP and the SS-FBLP-VSS estimation methods. These methods are compared with the maximum likelihood (ML) approach, the data-aided (DA) method, the pilot-aided (PA) scheme as well as the direct SVD method. From the plot it is seen that the SS-FBLP follows closely the performance of the direct SVD method. However, the SS-FBLP comes with a significantly lower computational cost. The SS-DBLP-VSS at $\alpha = 50$ offers a superior performance compared to the SS-FBLP and the SVD methods. This shows that along with the desired stability that the adaptive step-size offers, it also comes with a more favorable overall performance as compared to the other methods. Also, it can be seen from the plot that the SS-FBLP-VSS method at $\alpha = 50$ outperforms the DA method as well as the ML scheme. However, the pilot-aided technique, which is implemented with 8 pilots, outperforms the proposed methods. In terms of spectral efficiency, the proposed method is more attractive and desirable as the PA method comes with a higher overhead. A direct comparison of the proposed algorithms is as shown in Fig. 5. The methods are implemented with the linewidth set to 100 KHz and 400 KHz. Although the SS-FBLP-VSS

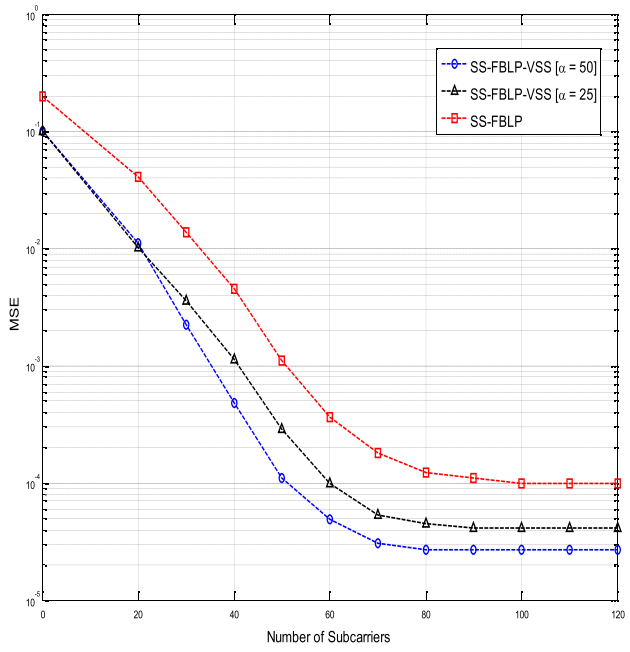

FIGURE 6. MSE plot showing the convergence behavior of the proposed algorithms.

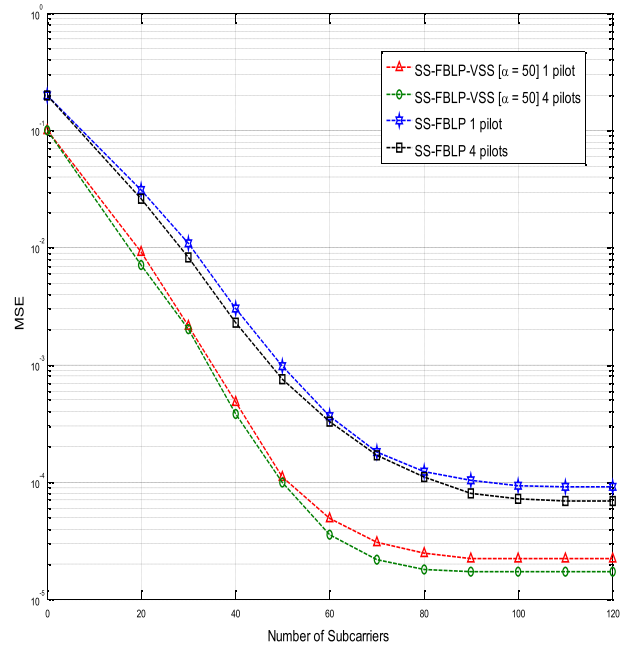

FIGURE 7. MSE plot showing the convergence behavior of the proposed algorithms with pilots.

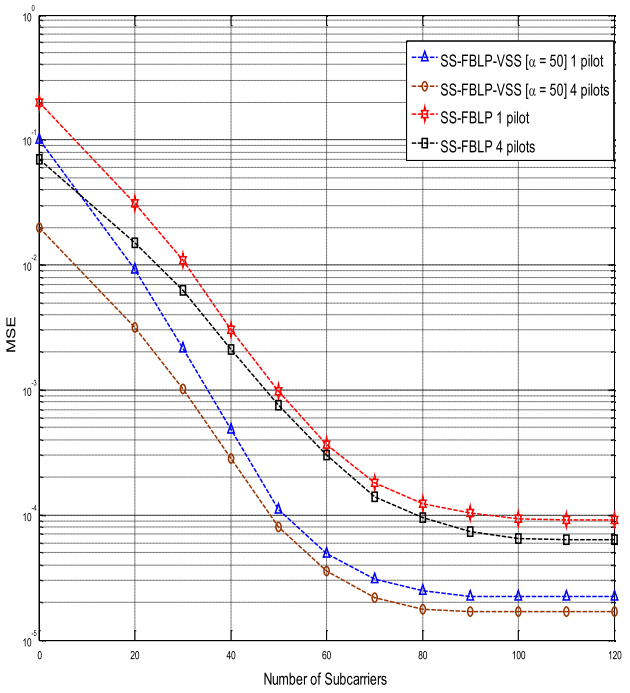

FIGURE 8. MSE plot showing the convergence behavior of the proposed algorithms with pilots.

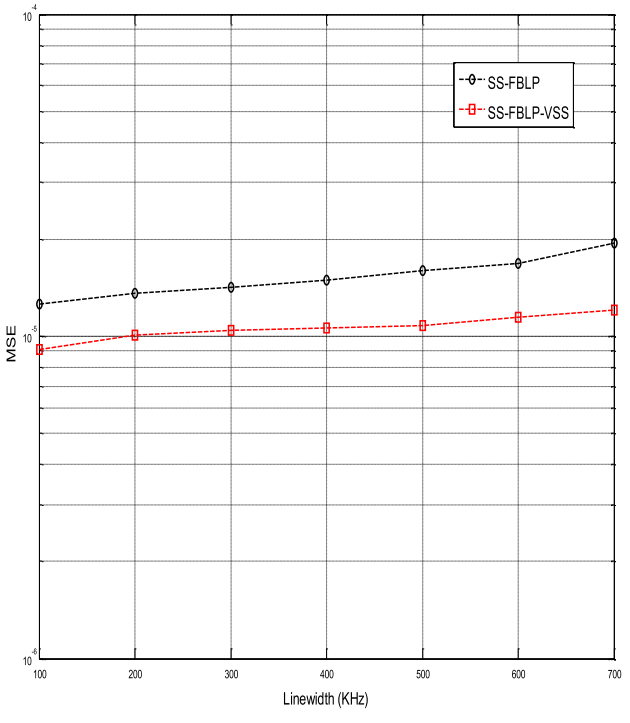

FIGURE 9. MSE versus linewidth plot for the proposed estimation algorithms.

clearly outperforms the SS-FBLP, both methods offer MSE performances, which are considerably stable across all SNR values.

In Fig. 6 and 7, the convergence behaviors of the proposed methods are shown. In addition, Fig. 7 also includes the performance of the algorithm using pilot subcarriers. From the plot, it can be seen that the MSE performance of the proposed methods decreases monotonically and then converges to a steady state. The SS-FBLP-VSS converges and attain steady-state faster than the SS-FBLP method. In Fig. 8, the initial value of the phase is set to the value of $\acute{B}(0)$ in (34), instead of initializing using a random value as in Fig. 7. It can be seen from the plots that Fig. 8 gives an enhanced

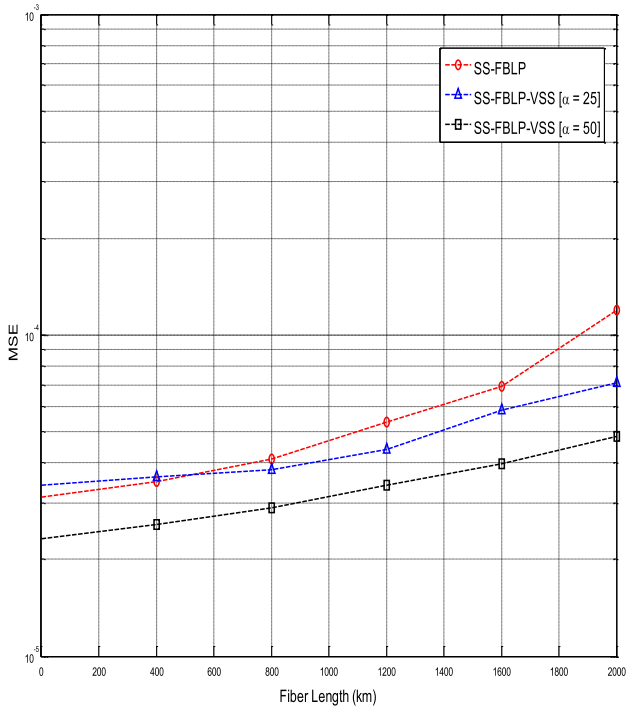

FIGURE 10. Performance of the proposed estimation algorithms with varying fiber length.

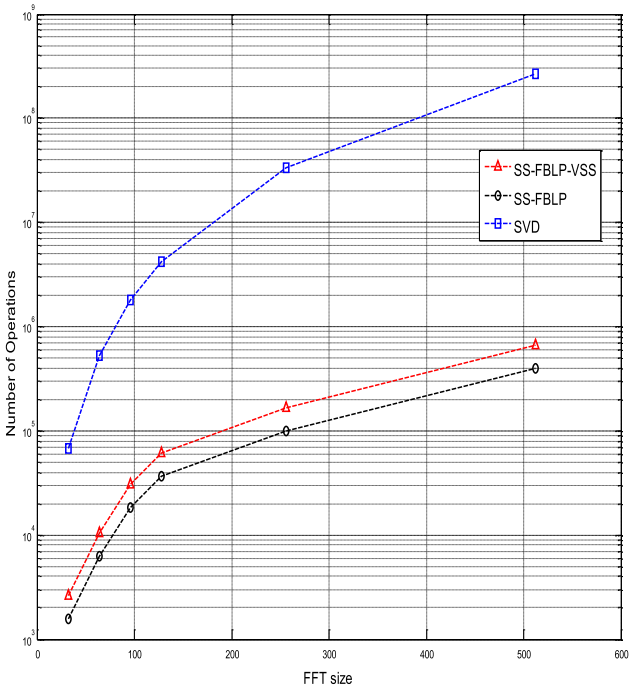

FIGURE 11. Complexity graph of the proposed schemes as compared to the SVD method.

performance using $\acute{B}(0)$ for the phase initialization. The variable step-size used, accounts for the excellent convergence behavior of the SS-FBLP-VSS method. Also, the superior MSE performance exhibited by the SS-FBLP-VSS method could be attributed to its fast convergence as a result of the adaptive step-size utilized instead of the fixed step-size used in the other method.

The proposed algorithms are executed in such a way that they can be compatible for future implementation in real-time digital signal processing (DSP) circuits. The specifications used in the simulations are similar to the ones used in the existing theoretical phase noise estimation schemes, which may not be efficiently compatible with existing DSP circuits. However, with improvements on the processing speed of these circuits, the proposed methods would be practically realizable with the aid of these emerging high-speed DSP circuits. In Fig. 9, the MSE versus the linewidth plot is shown. The performance of the SS-FBLP method is compared to the SS-FBLP-VSS method across different linewidth values. It is seen that both methods exhibit moderate robustness with increasing linewidth. Also, the graph in Fig. 10 shows the behavior of the proposed methods, as the length of the optical channel is increased. Although the performance of the proposed methods are affected, the methods especially the SS-FBLP-VSS method exhibits a rather graceful decline and fair stability across the distance.

VII. CONCLUSION

A blind estimation method, based on the subspace-tracking approach, has been proposed and implemented for phase noise estimation in CO-OFDM systems. The proposed SS-FBLP method is derived in such a way that the estimate of the phase noise, which is constantly changing over an OFDM frame, is achieved adaptively. The adaptive implementation is enhanced by employing the FBLP method, which ensures low complexity. Also, a variable step-size is introduced in the SS-FBLP-VSS method, to achieve better convergence and stability. Results show that the proposed methods perform considerably well in the practical CO-OFDM system utilized. The prosed methods achieve a superior performance as compared to the direct SVD method. Also, the results show that the SS-FBLP-VSS method offers an enhanced overall system performance compared to its SS-FBLP counterpart. Thus, in addition to the better convergence and stability that comes with the introduction of the adaptive step-size, an improved overall system performance is also achieved.

REFERENCES

[1] A. Barbieri, G. Colavolpe, T. Foggi, E. Forestieri, and G. Prati, "OFDM versus single-carrier transmission for 100 Gbps optical communication," *J. Lightw. Technol.*, vol. 28, no. 17, pp. 2537–2551, Sep. 1, 2010.

[2] I. B. Djordjevic and B. Vasic, "Orthogonal frequency division multiplexing for high-speed optical transmission," *Opt. Exp.*, vol. 14, no. 9, pp. 3767–3775, 2006.

[3] W. Shieh and C. Athaudage, "Coherent optical orthogonal frequency division multiplexing," *Electron. Lett.*, vol. 42, no. 10, pp. 587–589, May 2006.

[4] D. J. Ives, B. C. Thomsen, R. Maher, and S. J. Savory, "Estimating OSNR of equalised QPSK signals," *Opt. Exp.*, vol. 19, no. 26, p. B661–B666, 2011.

[5] G. Shen and M. Zukerman, "Spectrum-efficient and agile CO-OFDM optical transport networks: Architecture, design, and operation," *IEEE Commun. Mag.*, vol. 50, no. 5, pp. 82–89, May 2012.

[6] W. Shieh and I. Djordjevic, *OFDM for Optical Communications*. New York, NY, USA: Academic, 2010.

[7] X. Yi, W. Shieh, and Y. Tang, "Phase estimation for coherent optical OFDM," *IEEE Photon. Technol. Lett.*, vol. 19, no. 12, pp. 919–921, Jun. 15, 2007.

[8] S. T. Le, T. Kanesan, E. Giacoumidis, N. J. Doran, and A. D. Ellis, "Quasi-pilot aided phase noise estimation for coherent optical OFDM systems," *IEEE Photon. Technol. Lett.*, vol. 26, no. 5, pp. 504–507, Mar. 1, 2014.

[9] S. Cao, P. Y. Kam, and C. Yu, "Decision-aided, pilot-aided, decision-feedback phase estimation for coherent optical OFDM systems," *IEEE Photon. Technol. Lett.*, vol. 24, no. 22, pp. 2067–2069, Nov. 15, 2012.

[10] W. Shieh, "Maximum-likelihood phase and channel estimation for coherent optical OFDM," *IEEE Photon. Technol. Lett.*, vol. 20, no. 8, pp. 605–607, Apr. 15, 2008.

[11] S. Hussin, K. Puntsri, and R. Noé, "Performance analysis of RF-pilot phase noise compensation techniques in coherent optical OFDM systems," in *Proc. Eur. Conf. Netw. Opt. Commun.*, Jun. 2012, pp. 1–5.

[12] S. Randel, S. Adhikari, and S. L. Jansen, "Analysis of RF-pilot-based phase noise compensation for coherent optical OFDM systems," *IEEE Photon. Technol. Lett.*, vol. 22, no. 17, pp. 1288–1290, Sep. 1, 2010.

[13] S. Le, P. A. Haigh, A. D. Ellis, and S. K. Turitsyn, "Blind phase noise estimation for CO-OFDM transmissions," *J. Lightw. Technol.*, vol. 34, no. 2, pp. 745–753, Jan. 15, 2016.

[14] M. E. Mousa-Pasandi and D. V. Plant, "Zero-overhead phase noise compensation via decision-directed phase equalizer for coherent optical OFDM," *Opt. Express*, vol. 18, pp. 20651–20660, Sep. 2010.

[15] Y. Ha and W. Chung, "Non-data-aided phase noise suppression scheme for CO-OFDM systems," *IEEE Photon. Technol. Lett.*, vol. 25, no. 17, pp. 1703–1706, Sep. 1, 2013.

[16] T. Bo, L. Huang, and C. Chan, "Image processing based common phase estimation for coherent optical orthogonal frequency division multiplexing system," presented at the Opt. Fiber Commun. Conf., Los Angeles, CA, USA, 2015.

[17] T. Pfau, S. Hoffmann, and R. Noé, "Hardware-efficient coherent digital receiver concept with feedforward carrier recovery for M-QAM constellations," *J. Lightw. Technol.*, vol. 27, no. 8, pp. 989–999, Apr. 15, 2009.

[18] S. T. Le *et al.*, "Decision-directed-free blind phase noise estimation for CO-OFDM," presented at the Opt. Fiber Commun. Conf., Los Angeles, CA, USA, 2015.

[19] P. Comon and G. H. Golub, "Tracking a few extreme singular values and vectors in signal processing," *Proc. IEEE*, vol. 78, no. 8, pp. 1327–1343, Aug. 1990.

[20] I. Karasalo, "Estimating the covariance matrix by signal subspace averaging," *IEEE Trans. Acoust., Speech, Signal Process.*, vol. ASSP-34, no. 1, pp. 8–12, Feb. 1986.

[21] T. Chonavel, B. Champagne, and C. Riou, "Fast adaptive eigenvalue decomposition: A maximum likelihood approach," *IEEE Trans. Signal Process.*, vol. 83, no. 2, pp. 307–324, Feb. 2003.

[22] B. Champagne and Q.-G. Liu, "Plane rotation-based EVD updating schemes for efficient subspace tracking," *IEEE Trans. Signal Process.*, vol. 46, no. 7, pp. 1886–1900, Jul. 1998.

[23] B. Yang, "Projection approximation subspace tracking," *IEEE Trans. Signal Process.*, vol. 43, no. 1, pp. 95–107, Jan. 1995.

[24] B. Yang, "Asymptotic convergence analysis of the projection approximation subspace tracking algorithms," *IEEE Trans. Signal Process.*, vol. 50, nos. 1–2, pp. 123–136, Apr. 1996.

[25] J.-F. Yang and M. Kaveh, "Adaptive Eigensubspace algorithms for direction or frequency estimation and tracking," *IEEE Trans. Acoust., Speech, Signal Process.*, vol. ASSP-36, no. 2, pp. 241–251, Feb. 1988.

[26] E. Oja, "Principal components, minor components, and linear neural networks," *Neural Netw.*, vol. 5, no. 6, pp. 927–935, 1992.

[27] K. Abed-Meraim, S. Attallah, A. Chkeif, and Y. Hua, "Orthogonal Oja algorithm," *IEEE Signal Process. Lett.*, vol. 7, no. 5, pp. 116–119, May 2000.

[28] S. Attallah and K. Abed-Meraim, "Low-cost adaptive algorithm for noise subspace estimation," *Electron. Lett.*, vol. 38, pp. 609–611, Jun. 2002.

[29] T. Gustaffson and C. S. MacInnes, "A class of subspace tracking algorithms based on approximation of the noise-subspace," *IEEE Trans. Signal Process.*, vol. 48, no. 11, pp. 3231–3235, Nov. 2000.

[30] X. G. Doukopoulos and G. V. Moustakides, "Fast and stable subspace tracking," *IEEE Trans. Signal Process.*, vol. 56, no. 4, pp. 1452–1465, Apr. 2008.

[31] N. Rossi, P. Serena, and A. Bononi, "Polarization-dependent loss impact on coherent optical systems in presence of fiber nonlinearity," *IEEE Photon. Technol. Lett.*, vol. 26, no. 4, pp. 334–337, Feb. 15, 2014.

[32] N. Gisin and B. Huttner, "Combined effects of polarization mode dispersion and polarization dependent losses in optical fibers," *Opt. Commun.*, vol. 142, pp. 119–125, Oct. 1997.

[33] S. Wu and Y. Bar-Ness, "A phase noise suppression algorithm for OFDM-based WLANs," *IEEE Commun. Lett.*, vol. 6, no. 12, pp. 535–537, Dec. 2002.

[34] P. H. Moose, "A technique for orthogonal frequency division multiplexing frequency offset correction," *IEEE Trans. Commun.*, vol. 42, no. 10, pp. 2908–2914, Oct. 1994.

[35] X. Zhou, K. Long, R. Li, X. Yang, and Z. Zhang, "A simple and efficient frequency offset estimation algorithm for high-speed coherent optical OFDM systems," *Opt. Express*, vol. 20, no. 7, pp. 7350–7361, Mar. 2012.

[36] X. G. Doukopoulos and G. V. Moustakides, "Blind adaptive channel estimation in OFDM systems," *IEEE Trans. Wireless Commun.*, vol. 5, no. 7, pp. 1716–1725, Jul. 2006.

[37] F. Zhang, Y. Wang, and B. Ai, "Variable step-size MLMS algorithm for digital predistortion in wideband OFDM systems," *IEEE Trans. Consum. Electron.*, vol. 61, no. 1, pp. 10–15, Feb. 2015.

[38] D. W. Tufts and R. Kumaresan, "Estimation of frequencies of multiple sinusoids: Making linear prediction perform like maximum likelihood," *Proc. IEEE*, vol. 70, no. 9, pp. 975–989, Sep. 1982.

MUYIWA B. BALOGUN received the B.Sc. degree (Hons.) in electrical engineering from the University of Ilorin, Nigeria, in 2009, and the M.Sc. degree in electronic engineering from the University of KwaZulu-Natal in 2014. He is currently with the University of the Witwatersrand as a Doctoral Researcher. His research interests include signal processing, frequency synchronization algorithms for multicarrier systems, phase noise estimation, orthogonal frequency-division multiplexing systems, and optical transport networks.

OLUTAYO OYEYEMI OYERINDE received the B.Sc. (Hons.) and M.Sc. degrees in electrical and electronic engineering from Obafemi Awolowo University, Ile-Ife, Nigeria, in 2000 and 2004, respectively, and the Ph.D. degree in electronic engineering from the School of Engineering, University of KwaZulu-Natal (UKZN), Durban, South Africa, in 2010. He was a Post-Doctoral Research Fellow with the School of Engineering, UKZN, under UKZN Post-Doctoral Research Funding. He is currently a Telecommunications Lecturer with the School of Electrical and Information Engineering, University of the Witwatersrand, South Africa. His research interests are in the area of wireless communications including multiple antenna systems, orthogonal frequency-division multiplexing system and channels estimation, and signal processing techniques.

FAMBIRAI TAKAWIRA received the B.Sc. degree (Hons.) in electrical and electronic engineering from The University of Manchester, Manchester, U.K., in 1981, and the Ph.D. degree from Cambridge University, Cambridge, U.K., in 1984.

He has held various academic positions, including the Head of the School of Electrical, Electronic, and Computer Engineering and, just before his departure, the Dean of the Faculty of Engineering at the University of KwaZulu-Natal (UKZN), Durban, South Africa. He has also held appointments at the University of Zimbabwe, Harare, Zimbabwe; the University of California at San Diego, La Jolla, CA, USA; British Telecom Research Laboratories; and the National University of Singapore, Singapore. After 19 years at UKZN, in 2012, he joined the University of the Witwatersrand, Johannesburg, South Africa. His research interests include wireless communication systems and networks.

Dr. Takawira has served on several conference organizing committees. He served as the Communications Society Director for Europe, Middle East, and Africa region for the 2012–2013 term. He was an Editor of the IEEE TRANSACTIONS ON WIRELESS COMMUNICATIONS.